Applied Catalysis A, General 564 (2018) 64–71

Contents lists available at ScienceDirect

Applied Catalysis A, General

journal homepage: www.elsevier.com/locate/apcata

Elemental mercury catalytic oxidation removal and SeO_2 poisoning investigation over RuO_2 modified Ce-Zr complex

Songjian Zhao[a,b,1], Wanmiao Chen[a,c,1], Wenjun Huang[a], Jiangkun Xie[a], Zan Qu[a], Naiqiang Yan[a,*]

[a] School of Environmental Science and Engineering, Shanghai Jiao Tong University, 800 Dong Chuan Road, Shanghai, 200240, PR China
[b] School of Chemistry and Chemical Engineering, Shanghai Jiao Tong University, 800 Dong Chuan Road, Shanghai, 200240, PR China
[c] Shanghai Institute of Pollution Control and Ecological Security, Shanghai 200092, China

ARTICLE INFO

Keywords:
Elemental mercury
Ce-Zr solid solution
RuO_2
Catalytic mechanism
SeO_2

ABSTRACT

The mercury emission from coal-fired flue gas has drawn lots of attention worldwide. To achieve more efficient catalytic oxidation of Hg^0 in both high and low temperature, the RuO_2 modified Ce-Zr solid solution catalysts were prepared and evaluated at various conditions. It was found the polyvinylpyrrolidone (PVP) promoted $RuO_2/Ce_{0.6}Zr_{0.4}O_2$ catalyst displayed higher significant catalytic activity for Hg^0 oxidation. The mechanism of Hg^0 oxidation over $RuO_2/Ce_{0.6}Zr_{0.4}O_2$(PVP) was studied through various techniques, and Hg^0 oxidation approaches were found to consist of two steps: chemisorption process and regeneration process. The adsorbed Hg^0 was first oxidized with surface chemisorbed oxygen species to form HgO, which could desorb from the surface of catalysts by itself in absence of HCl. Also, the HgO could reacts with Cl^- in catalyst or adsorbed HCl to form $HgCl_2$, which could desorb into gas phase more readily. O_2 is indispensable for the chemisorption process. And the doping RuO_2 might have a synergistic effect with supporter, which could facilitate chemisorption process. Furthermore, SeO_2 poisoning of catalyst was investigated for the first time and found the existence of SeO_2 could slightly inhibit Hg^0 chemical adsorption process on the surface of the catalyst, while the regeneration process did not significantly affect.

1. Introduction

Mercury is a heavy metal pollutant with toxicity, bioaccumulation and persistence [1]. Superabundant anthropogenic emission of mercury into the atmosphere has attracted extensive attention worldwide and an international treaty (the *Minamata Convention on Mercury*) regarding mercury pollution was officially signed in 2013 [2,3]. Coal-fired power plants are primary anthropogenic mercury pollution sources in China and the United States due to their huge coal consumption. Mercury in coal-fired flue gas generally presents in three forms: elemental mercury (Hg^0), gaseous oxidized mercury (Hg^{2+}) and particulate-bound mercury (Hg^P), which mainly depends on the chlorine content of coal and combustion conditions [4]. Most of the oxidized and particulate-bound mercury can be readily captured with typical air pollution control devices (APCDs). However, Hg^0 is the dominant mercury species that escapes into the atmosphere from coal-fired flue gas due to the highly volatile and insoluble. Therefore, the catalytic oxidation of Hg^0 to Hg^{2+} with HCl from flue gas, is an economical way to obtain greater mercury removal efficiency with the existing APCDs [4–8], instead of additional particular equipment for mercury. For example, the catalysts involved in selective catalytic reduction (SCR) of NO_x process were investigated as potential Hg^0 conversion catalysts when sufficient HCl was present in flue gas [4,9]. However, the presence of ammonia (NH_3), employed as the SCR reductant, can significantly inhibit Hg^0 oxidation over conventional SCR catalysts [9,10]. Therefore, the oxidation of Hg^0 mainly occurs at the tail section of the SCR unit, which has lower NH_3 concentration.

In our previous study, a novel multi-functional catalyst (SCR-Plus) was proposed to be installed at the tail-end of SCR units [11], which would cooperate with SCR units to convert Hg^0 and unreacted ammonia simultaneously. Moreover, the low temperature SCR catalysts have drawn lots of attention and are a tendency in future industrial application. To cooperate with low temperature SCR catalysts, new catalyst which could convert elemental mercury and ammonia significantly at low temperature should be developed.

Recently, ceria(Ce)-zirconia(Zr) solid solution with cubic fluorite phase (Ce:Zr > 1:1), has been employed in many studies as catalyst carrier and drawn much attention ascribable to its excellent oxygen

* Corresponding author.
E-mail address: nqyan@sjtu.edu.cn (N. Yan).
[1] These two authors contributed equally to this work.

https://doi.org/10.1016/j.apcata.2018.07.022
Received 19 April 2018; Received in revised form 5 July 2018; Accepted 16 July 2018
Available online 17 July 2018
0926-860X/

storage capacity and outstanding redox properties [12,13]. Moreover, Ce-Zr solid solution supported metal oxide catalysts have served for De-NOx and display excellent performance for NO reduction [14]. Therefore, Ce-Zr solid solutions could be a promising catalyst carrier for the multi-functional (SCR-Plus) catalysts. What's more, it has been proposed in many studies that the oxidation of Hg^0 over catalysts with the presence of HCl might follow through Deacon reaction, in which HCl is converted to Cl_2 or Cl atom by oxygen [15–17]. And RuO_2 has been proven to be a very active component for Deacon reaction in many studies [18]. So RuO_2 is expected to be a potential catalyst component for Hg^0 conversion with the presence of HCl. In our previous research, we had already found that RuO_2 modified $Ce_{0.6}Zr_{0.4}O_2$ displayed significant catalytic activity for selective oxidation of NH_3 [19], but the activity of the RuO_2 modified $Ce_{0.6}Zr_{0.4}O_2$ on mercury oxidation is still unclear. Many mechanisms of mercury removal such as Mars-Maessen mechanism, Eley-Rideal mechanism and Langmuir-Hinshelwood mechanism [4,20,21], have been proposed for mercury oxidation over different catalysts [17]. However, the mechanism of mercury removal over RuO_2 modified $Ce_{0.6}Zr_{0.4}O_2$ has scarcely been clarified. Especially, the role of Cl in the process of elemental mercury oxidation is barely involved and remains indistinct. Thus, the mechanism of mercury oxidation is the main focus in this study.

Since Ru is usually considered as a noble metal and is more expensive than most of the transition metals, the content of RuO_2 was set at very low level (0.2%). To maintain the catalytic performance of the catalyst while using lower Ru content, sol-gel method with polyvinylpyrrolidone(PVP) was employed to enhance the dispersion of RuO_2 on catalyst surface.

Selenium (Se) is one of trace elements in coal during combustion. The average concentration of selenium in U.S. coals is 2.8 ppm [22]. When coal is burnt, more than 97% of Se in coal will be volatilized at 800 °C and existed with the form of SeO_2. About 637 t Se and 236 t As were introduced into atmosphere from coal combustion in China in 2009 [23]. Many studies have reported that As would make the catalyst deactivation [24], and Se in coal gas might have negative effect and due to the similar amount to As. However, there were no reports about the effect of SeO_2 poisoning for Hg^0 oxidation, so it was necessary to study the SeO_2 poisoning of catalysts.

In this study, elemental mercury removal efficiencies and adsorption behavior over various modified catalysts were evaluated. Also, possible catalytic mechanism of elemental mercury was studied, the role of RuO_2 and Cl in the oxidation was discussed especially. Moreover, the effect of SeO_2 poisoning of catalyst was investigated

2. Materials and methods

2.1. Preparation of catalysts

Please refer to the Supporting Information.

2.2. The loading method of SeO_2 poisoning

The catalyst nanoparticles were placed in the reactor with quartz wool firstly, and then some amount of SeO_2 were placed on the top of catalyst, which was purged by the flue gas with 4% O_2 and N_2 from top to bottom. And the furnace temperature raised slowly to 350 °C lasting for some time. The catalyst of loading was prepared and the sketch of SeO_2 loading shown in Supporting information (Fig. S1).

2.3. Catalytic activity measurement

The performance of the catalysts of Hg^0 adsorption and oxidation were tested in fixed-bed quartz reactor and the experiment system is shown in Supporting information (Fig. S2). The catalyst particles were placed in the reactor with quartz wool under atmospheric pressure, which was heated by a vertical electrical furnace. The feed gases were adjusted by mass flow controller and imported into the reactor with a total flow rate of 500 ml/min. The stable gas with elemental mercury from a permeation tube of Hg^0, flowed through the blank tube and the reactor tube to provide mercury signals. The mercury concentration was monitored by MD254 (LabTech) and Tekran 3300 mercury analyzer.

During mercury adsorption, the flow with Hg^0 firstly passed through the blank tube to provide original Hg^0 signal. After Hg^0 concentration was stable, the gas was switched to reactor tube to run the adsorption. For each Hg^0 catalytic oxidation experiment with HCl, the mercury contained gas was firstly introduced to pass the catalysts to undergo adsorption. After adsorption saturation was reached, the Hg^0 concentration in the outlet was measured as $[Hg^0]_1$. Then, the HCl or other gases was introduced into the gas and the Hg^0 concentration in the outlet was measured as $[Hg^0]_2$ until reaction equilibrium. The Hg^0 oxidation efficiency (E_{oxi}) over the catalysts was quantified by the following equation:

$$E_{oxi}(\%) = \frac{[Hg^0]_1 - [Hg^0]_2}{[Hg^0]_1} \times 100\%$$

3. Results and discussion

3.1. Catalytic activity

The catalytic oxidation efficiencies over catalysts were tested and evaluated under various conditions as shown in Fig. 1 (preliminary experiments showed the $Ce_{0.6}Zr_{0.4}O_2$ supported catalysts displayed superior catalytic activity). The Hg^0 oxidation efficiencies over $Ce_{0.6}Zr_{0.4}O_2$ are both lower than 10% at 350 °C and 150 °C. While, the mercury removal efficiency over $RuO_2/Ce_{0.6}Zr_{0.4}O_2$ increases to approximately 80% and 70% at high and low temperature, respectively, which indicates the doping of only 0.2% RuO_2 could significantly facilitate the Hg^0 conversion. Meanwhile, the synthesis method could also have an effect on the catalytic activities. The Hg^0 oxidation efficiency over $RuO_2/Ce_{0.6}Zr_{0.4}O_2$(PVP) increases to about 91% and 88% at high and low temperature, respectively. We propose that PVP might promote Ru dispersion over carrier just similar in other studies and the catalytic activity is enhanced in consequence [25]. Moreover, the effects of SO_2 on Hg^0 oxidation were tested and the results show that the Hg^0 removal efficiency is slightly restrained over all three catalysts at both high and low temperature. In addition, the Hg^0 oxidation efficiency of RuO_2/

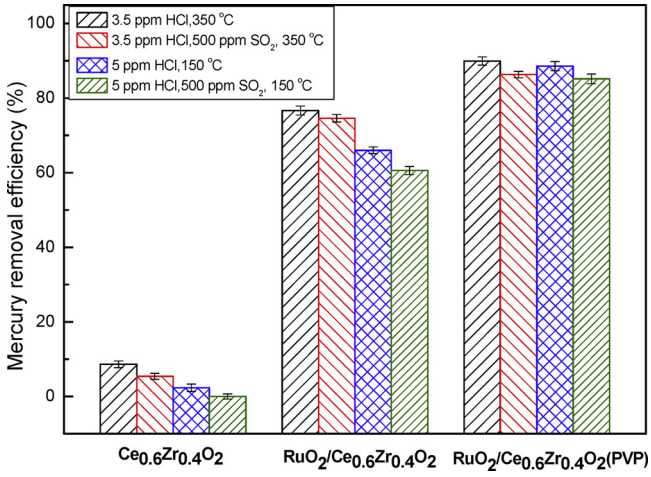

Fig. 1. The oxidation efficiencies of elemental mercury over various catalysts at different conditions.
The compositions in the gas were 4% O_2 and N_2. The Hg^0 concentration in the gas was approximately 110 (± 10) μg/m^3. The amount of catalysts were 60 mg and the space velocity (SV) was approximately 3.8 × 10^5 h^{-1}.

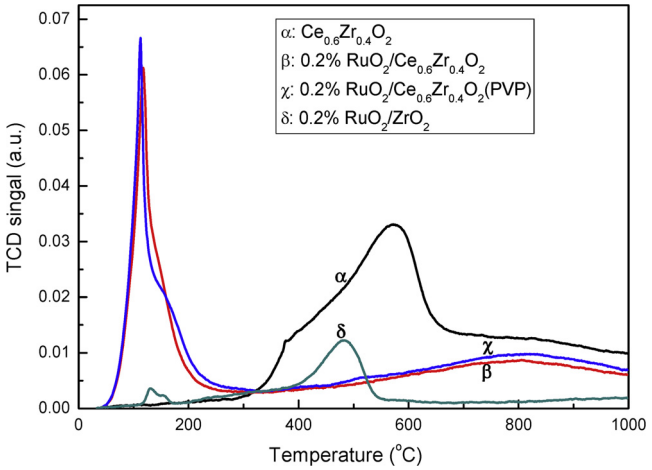

Fig. 2. H_2-TPR curves of $Ce_{0.6}Zr_{0.4}O_2$, $RuO_2/Ce_{0.6}Zr_{0.4}O_2$, $RuO_2/Ce_{0.6}Zr_{0.4}O_2$(PVP) and RuO_2/ZrO_2.
The H_2 (10%H_2/Ar) flow rate was 50 cm^3/min and the temperature ramp rate was 10 °C/min.

$Ce_{0.6}Zr_{0.4}O_2$(PVP) was greater than 95% in the simulated coal-fired flue gas (NO, NH_3, SO_2, H_2O, O_2 and N_2 balance) for long experimental duration (Fig. S3) and the results displayed catalysts had excellent durability for the complex components in flue gas.

3.2. H_2-TPR

To investigate the redox behavior of the catalysts, the temperature program reduction (TPR) by hydrogen for the $Ce_{0.6}Zr_{0.4}O_2$ and $RuO_2/Ce_{0.6}Zr_{0.4}O_2$ catalysts were tested. These results are shown in Fig. 2. In the $Ce_{0.6}Zr_{0.4}O_2$ catalyst, a board reduction peak centered at about 580 °C, which is attributed to the reduction of the Ce^{4+} in the Ce-Zr solid solution [26,27]. A very weak peak at 130 °C appeared on profile of 0.2%RuO_2/ZrO_2, and the peak is ascribed to the reduction of well-dispersed RuO_x species [28]. Since the ZrO_2 is very difficult to be reduced by H_2 at low temperature, the reduction peak about at 480 °C in profile of 0.2%RuO_2/ZrO_2 might be attributed to the interaction of Ru oxide and ZrO_2 support [28]. A strong peak appeared at about 110 °C over $RuO_2/Ce_{0.6}Zr_{0.4}O_2$ and $RuO_2/Ce_{0.6}Zr_{0.4}O_2$(PVP), which was much different with the profiles of $Ce_{0.6}Zr_{0.4}O_2$ and RuO_2/ZrO_2. This peak could not be attributed to the reduction of RuO_2 alone because content of RuO_2 is only 0.2% and the consumption of H_2 is much more than that of RuO_2/ZrO_2 (Table S1). Meanwhile, the large reduction peak at 580 °C caused by Ce^{4+} disappeared from profile of $RuO_2/Ce_{0.6}Zr_{0.4}O_2$, the strong peak at low temperature (about 110 °C) could be explained by the interaction between RuO_2 and catalyst support, which suggested Ru-Ce complex oxide might exist in the $RuO_2/Ce_{0.6}Zr_{0.4}O_2$ catalyst and the oxidation capacity at low temperature was significantly improved. And this might explain the results that efficiencies of mercury oxidation were much higher with the presence of RuO_2.

3.3. Hg^0 adsorption

As we know, catalytic reaction is generally associated with adsorption. Therefore, to clarify the mechanism of mercury oxidation over the RuO_2 modified catalysts, the adsorption of Hg^0 over various conditions were investigated and the results are shown in Fig. 3. Firstly, the fresh $RuO_2/Ce_{0.6}Zr_{0.4}O_2$ was tested until equilibrium and the adsorption capacity for Hg^0 was 1.36 mg/g (curve A). After that, the Hg^0 was suspended and the catalyst was purged with O_2 and N_2 balance for 2 h. Afterwards, the adsorption experiment of Hg^0 was carried again over the purged catalyst and the adsorption curve was obtained as curve B in Fig. 3. As shown in result, the adsorption time was shortened and the

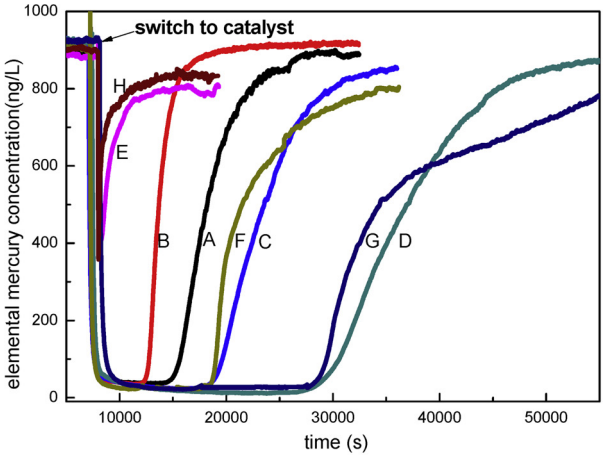

(a)

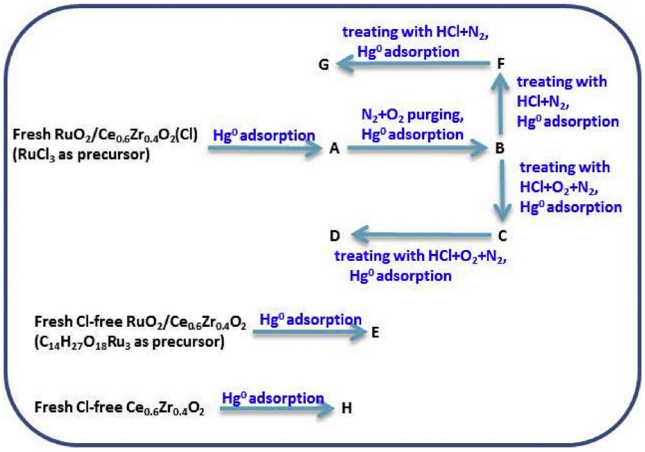

(b)

Fig. 3. (a) The adsorption curves of elemental mercury over various catalysts at 350 °C (b) The order of the adsorption experiment in Fig. 3(a).
The space velocity (SV) was approximately 3.0×10^5 h^{-1}. The total flow rate was set at 500 ml/min. The amount of catalysts were 60 mg. Temperature was 350 °C. Treating with HCl + N_2: Mercury suspend, catalyst was treated with 15 ppm HCl + N_2 for 90 min and then purged with N_2 for 30 min. Treating with HCl + O_2 + N_2: Mercury suspend, catalyst was treated with 15 ppm HCl + 4% O_2 + N_2 for 90 min and then purged with 4%O_2 + N_2 for 30 min.

capacity regenerated to 0.84 mg/g, which meant portion of adsorbed mercury could desorb from the catalyst surface during purging and some active adsorption sites on the surface were regenerated. Then, the catalyst was treated under 15 ppm HCl, 4% O_2 and N_2 balance for 90 min and 4% O_2 and N_2 balance for 30 min to remove physical absorbed HCl, respectively. After the treatment, the Hg^0 adsorption over the catalyst was carried again and the adsorption curve was curve C. The results showed that the adsorption capacity of $RuO_2/Ce_{0.6}Zr_{0.4}O_2$ was recovered and even promoted to 2.16 mg/g by HCl. After that, the catalyst was treated with HCl again and the adsorption curve could be acquired as curve D, which showed that the adsorption capacity of $RuO_2/Ce_{0.6}Zr_{0.4}O_2$ for Hg^0 was recovered and increased significantly to 3.92 mg/g, approximately 3 times compared with fresh catalyst. Since Cl in catalysts would have important effects on mercury removal (both adsorption and catalysis), the adsorption experiment was carried over fresh Cl-free $RuO_2/Ce_{0.6}Zr_{0.4}O_2$ and $Ce_{0.6}Zr_{0.4}O_2$ catalyst and the adsorption capacity was only 0.2 and 0.11 mg/g, which was much lower than normal $RuO_2/Ce_{0.6}Zr_{0.4}O_2$ which contains Cl and indicated that chlorine played a significant role in Hg^0 adsorption (discuss later).

Deacon Reaction mechanism in which HCl was firstly oxidized with O_2 to form Cl atom, was proposed to explain catalytic oxidation of

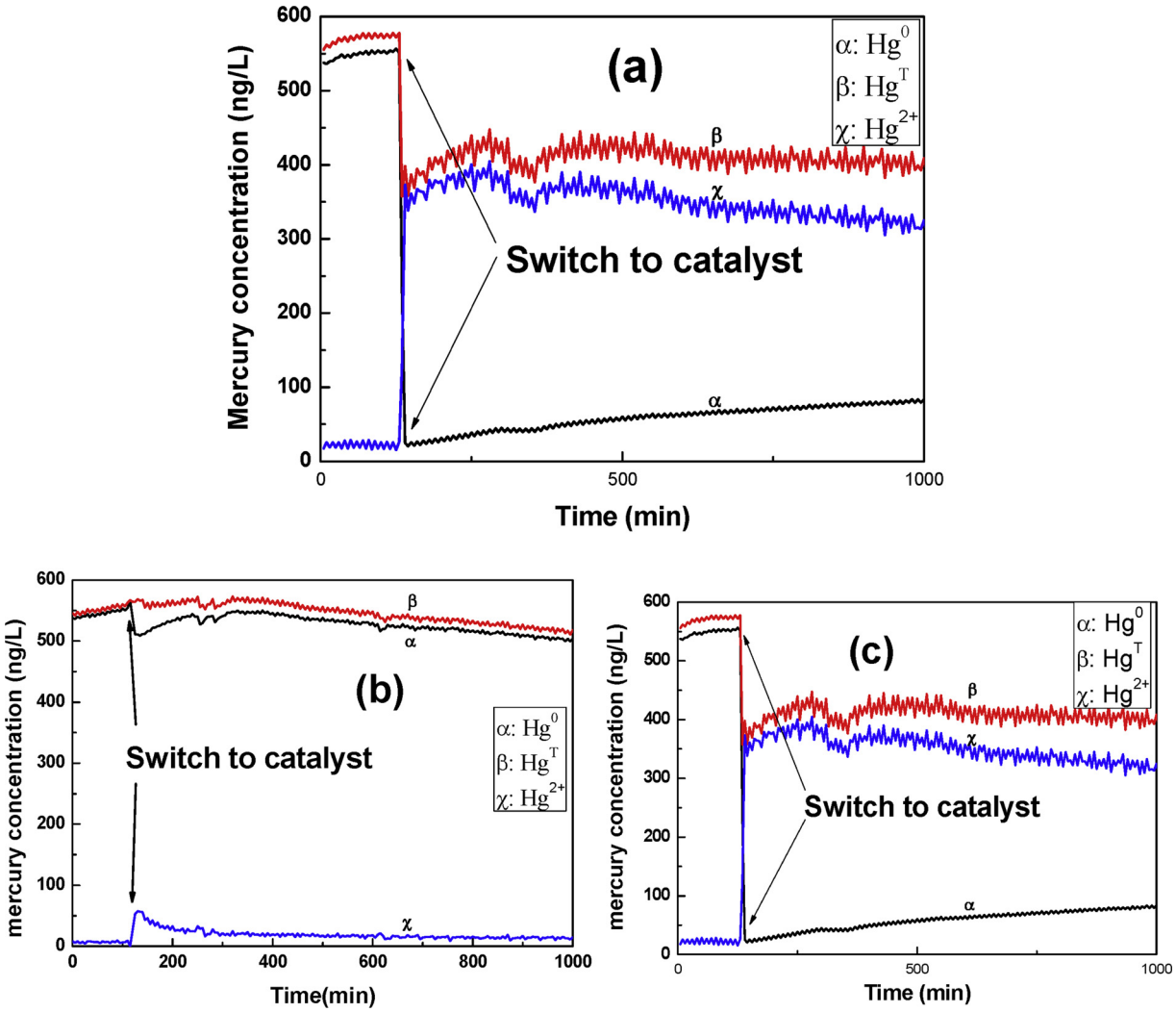

Fig. 4. Mercury adsorption over catalysts monitored with Terkan mercury analyzer.
The space velocity (SV) was approximately 9.1 × 10^5 h^{-1}. The amount of catalysts was 25 mg. The temperature was 350 °C. (a) $RuO_2/Ce_{0.6}Zr_{0.4}O_2$, 4%$O_2$ and N_2 (b) $RuO_2/Ce_{0.6}Zr_{0.4}O_2$, N_2 (c) Cl-free $RuO_2/Ce_{0.6}Zr_{0.4}O_2$, 4%$O_2$ and N_2.

mercury in many studies [15–17]. Also, to evaluate the role of O_2 and interaction between HCl and O_2, another adsorption experiment was carried over the fresh $RuO_2/Ce_{0.6}Zr_{0.4}O_2$ catalyst. After the treating under 15 ppm HCl and N_2 without O_2, the adsorption capacity was also regenerated (curve F and G) and the adsorption curves were similar with results under HCl, 4% O_2 and N_2, which indicates that O_2 is not necessary for the regeneration process with HCl. Since HCl could have effects without O_2, which implies that Deacon reaction mechanism may not be appropriate explanation for mercury oxidation in this research. These results indicate that the elemental mercury oxidation over the $RuO_2/Ce_{0.6}Zr_{0.4}O_2$ catalyst consist of two separable process, the Hg^0 adsorption process and the regeneration process with HCl.

To further investigate the adsorption of mercury over RuO_2 modified catalysts, the Tekran mercury analyzer which could directly monitor Hg^0 and Hg^T simultaneously, was employed to detect the adsorption process and the results are shown in Fig. 4. Some amount of oxidized mercury (Hg^{2+}) was generated when the Hg^0 passed through the RuO_2 modified catalyst with $RuCl_3$ as precursor (Fig. 4(a)) and it demonstrated that elemental mercury could be oxidized without gaseous HCl. The result in Fig. 4(b) was acquired by carrying the Hg^0 adsorption without O_2 over RuO_2 modified catalyst with $RuCl_3$ as precursor. Only little amount of oxidized mercury was detected during the initial stage of adsorption, which could be oxidized by surface chemisorbed oxygen in the catalysts (discuss later). The results prove that adsorption and oxidation of mercury are negligible without O_2. Similar experiment was carried out over the Cl-free $RuO_2/Ce_{0.6}Zr_{0.4}O_2$ ($C_{14}H_{27}O_{18}Ru_3$ as precursor) and the results are shown in Fig. 4(c). Elemental mercury could still be oxidized over the Cl-free $RuO_2/Ce_{0.6}Zr_{0.4}O_2$ catalyst with O_2, but the oxidized mercury (Hg^{2+}) concentration was much less compared with that of catalyst with $RuCl_3$ as precursor and elemental mercury slipping from the catalyst was much higher. It could be inferred from the results that O_2 is indispensable for mercury adsorption, and elemental mercury is firstly adsorbed and oxidized with O_2 on the catalyst and then the oxidized mercury (Hg^{2+}) desorbed from the surface of catalyst. The Cl^- in catalyst is not necessary for the mercury oxidation, but it could promote oxidation of Hg^0.

3.4. Mechanism of catalytic oxidation of Hg^0

To further determine the mechanism of elemental mercury oxidation, the catalytic oxidation of Hg^0 with HCl was also carried out and monitored by the Tekran mercury analyzer. As the result in Fig. S4 shows, when some amount of mercury (about 110 ng/L) passed through the $RuO_2/Ce_{0.6}Zr_{0.4}O_2$(PVP), approximately 68 ng/L oxidized mercury (Hg^{2+}) could be detected in the gas. And when the HCl was added into the gas, the total mercury (Hg^T) concentration increased to about 136 ng/L rapidly. Afterthat, the Hg^T decreased rapidly to about 77 ng/

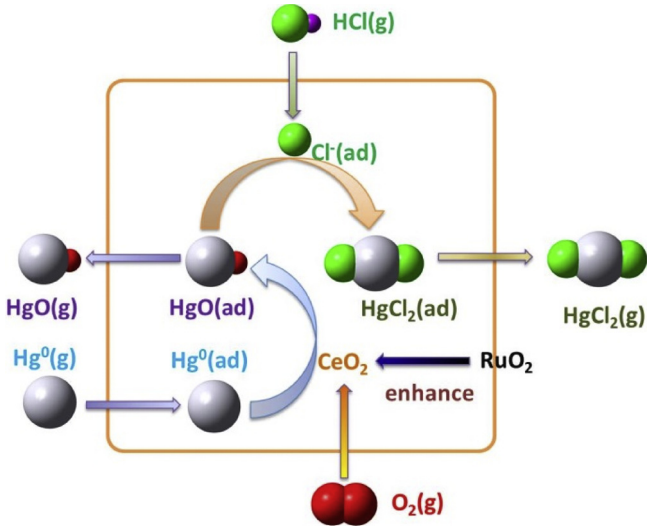

Fig. 5. Mechanism of mercury oxidation over $RuO_2/Ce_{0.6}Zr_{0.4}O_2$.

L, and then increased slowly. When HCl was introduced into the gas, portion of the HgO on the surface of the catalyst could react with HCl to form $HgCl_2$ and desorbed from the surface, which led the momentary increase of Hg^T. Since desorption of the oxidized mercury was accelerated and the active adsorption sites on the surface were regenerated by HCl, the adsorption (both physical and chemical) of elemental mercury was enhanced. In this way, the concentration of the elemental mercury in gas decreased to very low level as shown in Fig. S4 and the Hg^T also reduced to some degree. When the reaction equilibrium was researched, the Hg^T recovered to original concentration (about 110 ng/L) and the mercury was balanced during the catalytic reaction.

Above all, the catalytic oxidation of elemental mercury on the surface with the presence of HCl contains two separate steps: chemisorption process and the regeneration process (as shown in Fig. 5). Firstly, the Hg^0 in gas is adsorbed to the surface of the catalysts and adsorbed Hg^0 then is oxidized to Hg^{2+} by the active oxygen species from metallic oxides catalysts (Reactions (1) and (2)). The O 1s XPS spectrum on catalyst after Hg^0 adsorption without O_2 and fresh catalyst are shown in Fig. S5. The peak at 529.5 eV might be ascribed to lattice oxygen, and the peak at 531.4 eV could be attributed to surface chemisorbed oxygen [29]. Besides, the peak at 529.5 eV was nucleophilic states, and 531.4 eV peak denoted electrophilic states for the O 1s which was beneficial for oxidation reaction [30]. And it was found in the XPS results that the ratio of surface chemisorbed oxygen on catalyst decreased from 29.1% to 20.4% after Hg^0 adsorption without O_2, which displayed that the adsorbed Hg^0 was oxidized by the surface chemisorbed oxygen species.

The adsorption of elemental mercury on $Ce_{0.6}Zr_{0.4}O_2$ without HCl is shown in Fig. S6, and the conversion of Hg^0 is much lower than that of $RuO_2/Ce_{0.6}Zr_{0.4}O_2$(PVP) in absence of HCl. This result displayed that the doping of RuO_2 could facilitate the chemisorption process because the oxidation ability of the catalyst is enhanced as shown in H_2-TPR results. Also, some studies proposed that O_2 was more easily be dissociated with the presence of RuO_2, which might accelerate the replenishing of surface chemisorbed oxygen and result in superior chemisorption [31]. The chemisorption process could occur without chlorine (neither gasous HCl nor Cl^- on surface), but the O_2 in gas is essential for this step. When no chlorine exists in the catalysts or gas, the oxidized mercury could also desorb from the surface of the catalysts (Reaction (3)). This reaction pathway could explain the results in Fig. S4 that elemental mercury could still be oxidized by the catalysts in absence of HCl.

$$Hg^0(g) \rightarrow Hg^0(ads) \quad (1)$$

$$Hg^0(ads) + O \rightarrow HgO(ads) \quad (2)$$

$$HgO(ads) \rightarrow HgO(g) \quad (3)$$

$$HCl(g) \rightarrow HCl(ads) \quad (4)$$

$$HgO(ads) + 2HCl(ads) \rightarrow HgCl_2(ads) + H_2O \quad (5)$$

$$HgCl_2(ads) \rightarrow HgCl_2(g) \quad (6)$$

$$Hg + 2HCl + O_2 \rightarrow HgCl_2 + H_2O \quad (7)$$

When HCl exists in the gas, the oxidized mercury could react with the adsorbed HCl and $HgCl_2$ is generated (Reactions (5) and (6)). Since the $HgCl_2$ could more readily desorb from the surface of the catalysts, the regeneration of active sites on the catalysts are accelerated by the HCl. It had already been proven in research that the presence of HCl could facilitate the release of oxidized mercury into gas phase [32]. The Cl^- in catalyst could also expedite the release of oxidized mercury into the gas phase and regeneration of active adsorption sites, and this could explain the results in Fig. 3 that the adsorption capacity of Hg^0 over $RuO_2/Ce_{0.6}Zr_{0.4}O_2$ was improved significantly by HCl treatment. What's more, the effects of Cl could explain the results that the oxidation efficiencies of elemental mercury were much higher in presence of HCl.

3.5. The effect of SeO_2 on Hg^0 catalytic oxidation

In order to study the loading of SeO_2, X-ray fluorescence (XRF) analysis was performed for different catalysts loaded with SeO_2 and the results are shown in Table S2. All the results in the table are based on 30 mg of the catalyst, using different SeO_2 loading amount. The Se content in the table indicates the result by the XRF test, and the Se adhesion ratio indicates the ratio of actual test Se content and theoretically Se content assumed all SeO_2 attached the catalyst. It can be seen that with the increase of the amount of SeO_2 loading amount, the adhesion ratio of Se does not significantly increase or decrease, which are fluctuated within a relatively small range of 15%–20%, indicated that the load ratio of SeO_2 is basically kept at a relatively stable level during the experimental process and can be used to research the Hg^0 catalytic oxidation.

Fig. S7 shows the effect of SeO_2 on Hg^0 catalytic oxidation. The fresh catalyst had a high Hg^0 catalytic oxidation efficiency, with 99% at 5 ppm HCl. However, the oxidation efficiency reduced after loading SeO_2 on $RuO_2/Ce_{0.6}Zr_{0.4}O_2$(PVP). With the amount increase of SeO_2, the Hg^0 oxidation efficiency declined slowly until loading 5 mg SeO_2. And then when the loading amount of SeO_2 reached 9 mg, the catalytic performance of $RuO_2/Ce_{0.6}Zr_{0.4}O_2$ had no obviously variation with the increase of SeO_2. It indicated that SeO_2 was bad for the Hg^0 catalytic oxidation, and might inhibit the oxidation reaction process.

The effect of SO_2 on $RuO_2/Ce_{0.6}Zr_{0.4}O_2$(PVP) poisoning by SeO_2 was also studied. It can be seen that SO_2 had an inhibitory effect for Hg^0 catalytic oxidation, which might be possibly that SO_2 is adsorbed at the active site, inhibiting the reaction of Hg^0 and chlorine species. While the effect reduced when the loading amount of SeO_2 was above 5 mg, which might because the poisoning mechanism of SeO_2 and SO_2 was similar due to the same family of Se and S elements. And when the amount of SeO_2 was high, the active site SO_2 attached was little, so the influence of SO_2 is relatively small.

The pathway of elemental mercury oxidation over the $RuO_2/Ce_{0.6}Zr_{0.4}O_2$ catalyst consists of two steps above: chemisorption process and regeneration process. So the effect of SeO_2 on the two steps was studied, respectively.

3.5.1. The effect of SeO_2 for Hg^0 chemisorption process

Fig. S8 shows the adsorption curves of fresh and SeO_2 poisoned

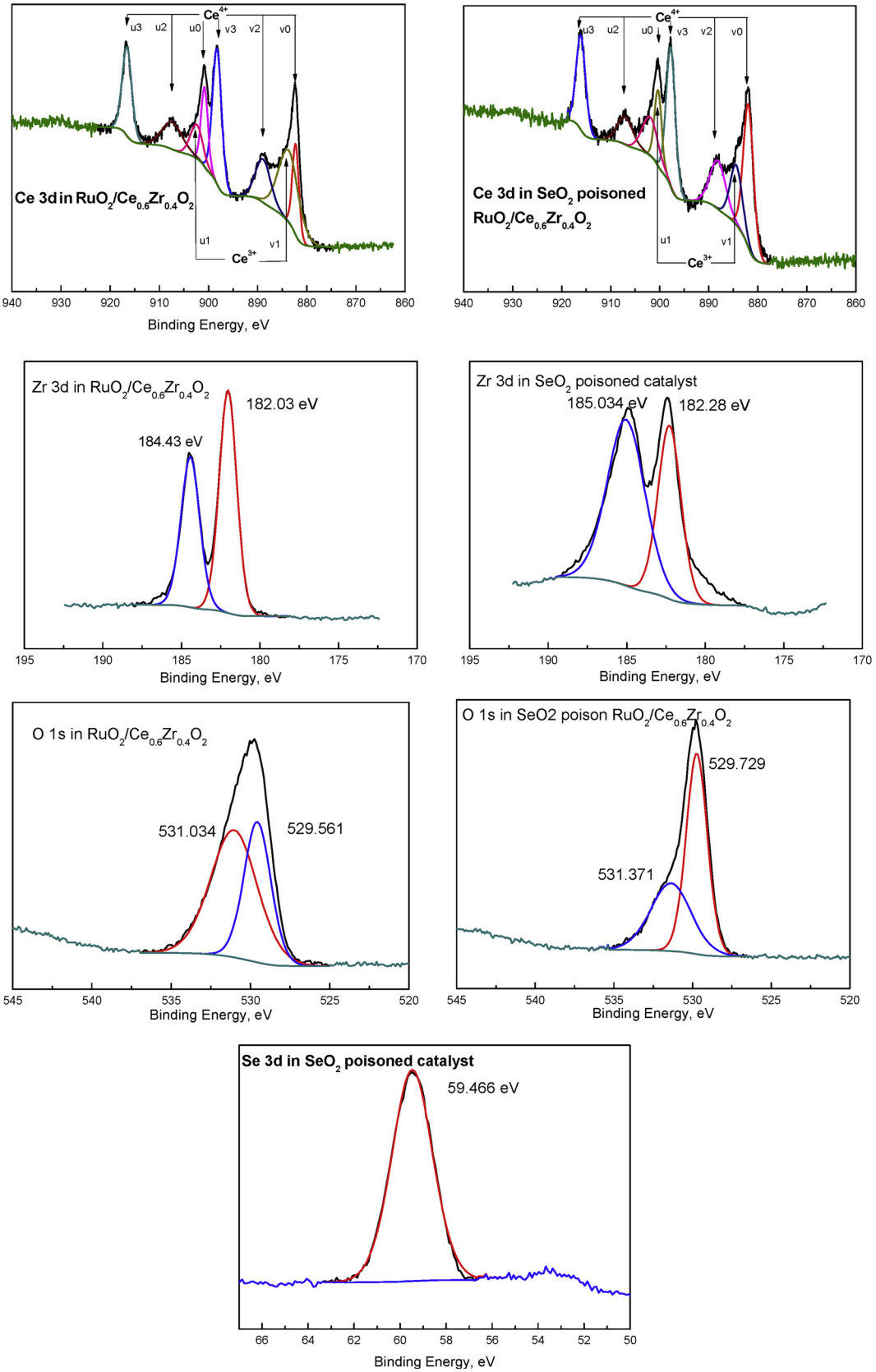

Fig. 6. The Ce XPS spectrum of fresh and SeO_2 poisoned $RuO_2/Ce_{0.6}Zr_{0.4}O_2$(PVP) catalysts.

$RuO_2/Ce_{0.6}Zr_{0.4}O_2$(PVP) catalysts. As can be seen from Fig. S8, fresh catalyst had a certain Hg^0 adsorption ability, but not high. The concentration of Hg^0 presented a trend increasing earlier and then decreasing, and reached about 70% of initial mercury concentration, indicated the oxidation efficiency was about 30%. When Hg^0 was passed through SeO_2 poisoned catalyst, the Hg^0 concentration

presented the similar variation tendency compared with that of fresh catalyst. After reaching reaction equilibrium, Hg^0 concentration accounted for about 77% of initial mercury concentration, manifested the Hg^0 oxidation efficiency was about 23%, lower than fresh catalyst. It suggested that SeO_2 would affect the chemisorption mechanism.

3.5.2. The effect of SeO_2 for regeneration process

The adsorption curves of HCl treated fresh and SeO_2 poisoned were studied, shown in Fig. S9. Consistent with results of Fig. 3, the Hg^0 adsorption ability of fresh $RuO_2/Ce_{0.6}Zr_{0.4}O_2$ enhanced obviously due to the HCl treatment, and Hg^0 removal efficiency reach above 90% within 250 min. SeO_2 poisoned catalyst had the similar Hg^0 adsorption ability, indicated that SeO_2 had little effect on the process of HCl adsorption and combination with HgO into $HgCl_2$.

Through the above two adsorption experiment, as can know SeO_2 poisoning can slightly inhibit Hg^0 chemical adsorption process on the surface of the catalyst, the reaction of (1)–(3) was affected negatively. While the regeneration process did not significantly affect, manifested that the reaction of (4) and (5) can be proceeded normally for SeO_2 poisoned catalyst.

3.5.3. The analysis of poisoned mechanism

To investigate the effect of SeO_2 poisoning for redox ability of catalyst, H_2-TPR experiment of fresh and poisoned catalyst was operated, shown in Fig. S10. The reduction peak of Ce-Zr and $0.2\%RuO_2/Ce_{0.6}Zr_{0.4}O_2$ were mentioned in Fig. S10. And the reduction peaks of SeO_2 poisoned catalyst presented different peak position and shape compared with fresh catalyst. Firstly, the strong peak located at about 110 °C disappeared, which was assigned to the interaction between RuO_2 and catalyst support. And there was a board peak started from 200 °C, and the peak value was located at about 470 °C with shoulder peak at about 300 °C. It indicated that the loading SeO_2 changed obviously the redox ability of catalyst. The strong peak at 470 °C might be due to the interaction of Se and Ce oxide, while the shoulder peak can be attributed to the composite oxide of Ru and Se. The results of TPR indicated that SeO_2 poisoning reduced the oxidation ability of catalyst at low temperature, so that the Hg^0 chemisorption was worse.

The XPS spectrum of fresh and SeO_2 poisoned $RuO_2/Ce_{0.6}Zr_{0.4}O_2$(PVP) catalysts were analyzed to study the chemical valence variation of element due to the SeO_2 poisoning, shown in Fig. 6. The XPS spectrum of Zr 3d (Fig. 6(a)) can be deconvoluted into two peaks for Zr 3d5/2 and Zr 3d3/2, located at around 182.5 eV and 185 eV respectively, which was attributed to the zirconium in the Zr^{4+} state [33]. After loading SeO_2, the proportion of characteristic peak at 184.7 eV increased from approximately 42% to 61%, indicated that the existing form of Zr was affected by SeO_2.

The CeO_2 spectrum was composed of two multiplets (v and u), where V and U correspond to the spin-orbit split 3d 5/2 and 3d 3/2 core holes, respectively. The peaks referred to as u0, u2, u3, v0, v2, v3 are contributed by CeO_2 and assigned to Ce IV ($3d^{10}4f^0$), while the peak of u1 and v1 are assigned to Ce III ($3d^{10}4f^1$) [34]. The proportion of $Ce^{3+}/(Ce^{3+} + Ce^{4+})$ could calculate by the area of these peaks. The proportion of Ce^{3+} of $RuO_2/Ce_{0.6}Zr_{0.4}O_2$ were approximately 30%, which was reduced to 20% after loading. And the existence of Ce^{3+} can induce the charge imbalance cavitation and unsaturated bonds, which can make the chemical adsorption of oxygen on the surface of catalyst increase and promote the catalytic activity.

It can be seen from Fig. 6 the proportion of chemical adsorption of oxygen decreased from approximately 61% to 39% when loading SeO_2. The analysis above has shown that Hg^0 chemisorption process primarily depended on the surface adsorption oxygen. And the results of XPS spectrum show that the existence of SeO_2 could suppress the Hg^0 chemical adsorption activity of catalyst, consistent with the results in Fig. S8.

4. Conclusions

In conclusion, the PVP promoted $0.2\%RuO_2$ modified $Ce_{0.6}Zr_{0.4}O_2$ catalyst displayed excellent catalytic oxidation activity for elemental mercury with various conditions at both high and low temperature. The pathway of elemental mercury oxidation over the $RuO_2/Ce_{0.6}Zr_{0.4}O_2$ catalyst was found to consist of two steps: chemisorption process and regeneration process. That is the adsorbed Hg^0 is first oxidized with surface chemisorbed oxygen species to form HgO. The HgO could desorb from the surface of catalysts in absence of HCl. And also, the HgO could reacts with Cl^- from surface of catalyst or adsorbed HCl to form $HgCl_2$, which is more readily to desorb into the gaseous phase. O_2, which could replenish the consumption of surface chemisorbed oxygen, is indispensable for the chemisorption process. And the doping of RuO_2 could have synergistic effect with supporter and facilitate chemisorption process, which led the results that RuO_2 modified catalysts displayed significant performance for elemental mercury removal. Besides, loading SeO_2 can slightly inhibit Hg^0 chemical adsorption process on the surface of the catalyst, while the regeneration process did not significantly affect.

Acknowledgments

This study was supported by the National Key Research and Development Program of China (No. 2017YFC0210500) and the National Natural Science Foundation of China (No. 21677096), (No. 21607102) and (No. U1662132), and China's Post-doctoral Science Fund (No. 2015M581626) and (No. 2017M621484), and this research is funded by the Hong Kong Scholars Program.

Appendix A. Supplementary data

Supplementary material related to this article can be found, in the online version, at doi:https://doi.org/10.1016/j.apcata.2018.07.022.

References

[1] A.A. Presto, E.J. Granite, Environ. Sci. Technol. 41 (2007) 6579–6584.
[2] A.A. Presto, E.J. Granite, A. Karash, Ind. Eng. Chem. Res. 46 (2007) 8273–8276.
[3] R. Kessler, Environ. Health Perspect. 121 (2013) A304.
[4] A.A. Presto, E.J. Granite, Environ. Sci. Technol. 40 (2006) 5601–5609.
[5] Y.J. Wang, Y. Liu, Z.B. Wu, J.S. Mo, B. Cheng, J. Hazard. Mater. 183 (2010) 902–907.
[6] X. Li, J.Y. Lee, S. Heald, Fuel 93 (2012) 618–624.
[7] Q. Wan, L. Duan, K. He, J. Li, Chem. Eng. J. 170 (2011) 512–517.
[8] Y. Liu, Y. Wang, H. Wang, Z. Wu, Catal. Commun. 12 (2011) 1291–1294.
[9] S. Niksa, N. Fujiwara, J. Air Waste Manage. 55 (2005) 1866–1875.
[10] C.L. Senior, J. Air Waste Manage. 56 (2006) 23–31.
[11] W. Chen, Y. Ma, N. Yan, Z. Qu, S. Yang, J. Xie, Y. Guo, L. Hu, J. Jia, Fuel 133 (2014) 263–269.
[12] Q. Wang, B. Zhao, G. Li, R. Zhou, Environ. Sci. Technol. 44 (2010) 3870–3875.
[13] L. Chen, J. Li, M. Ge, J. Phys. Chem. C 113 (2009) 21177–21184.
[14] J.H. Ko, S.H. Park, J.-K. Jeon, S.-S. Kim, S.C. Kim, J.M. Kim, D. Chang, Y.-K. Park, Catal. Today 185 (2012) 290–295.
[15] K.C. Galbreath, C.J. Zygarlicke, Fuel Process. Technol. 65 (2000) 289–310.
[16] X. Li, Z. Liu, J. Kim, J.-Y. Lee, Appl. Catal. B 132 (2013) 401–407.
[17] W. Xu, H. Wang, X. Zhou, T. Zhu, Chem. Eng. J. 243 (2014) 380–385.
[18] D. Teschner, G. Novell-Leruth, R. Farra, A. Knop-Gericke, R. Schlögl, L. Szentmiklósi, M.G. Hevia, H. Soerijanto, R. Schomäcker, J. Pérez-Ramírez, Nat. Chem. 4 (2012) 739–745.
[19] W. Chen, Y. Ma, Z. Qu, Q. Liu, W. Huang, X. Hu, N. Yan, Environ. Sci. Technol. 48 (2014) 12199–12205.
[20] A.A. Presto, E.J. Granite, Platin. Met. Rev. 52 (2008) 144–154.
[21] E.J. Granite, H.W. Pennline, R.A. Hargis, Ind. Eng. Chem. Res. 39 (2000) 1020–1029.
[22] R.B. Finkelman, C.A. Palmer, P. Wang, Int. J. Coal Geol. 185 (2018) 138–160.
[23] J. Chen, G. Liu, Y. Kang, B. Wu, R. Sun, C. Zhou, D. Wu, Chemosphere 90 (2013) 1925–1932.
[24] M. Kong, Q. Liu, X. Wang, S. Ren, J. Yang, D. Zhao, W. Xi, L. Yao, Catal. Commun. 72 (2015) 121–126.
[25] T. Yu, J. Zeng, B. Lim, Y. Xia, Adv. Mater. 22 (2010) 5188–5192.
[26] Y. Guo, G. Lu, Z. Zhang, S. Zhang, Y. Qi, Y. Liu, Catal. Today 126 (2007) 296–302.
[27] L. Zhi Min, W. Jian Li, Z. Jun Bo, C. Yao Qiang, Y. Sheng Hui, G. Mao Chu, J. Hazard. Mater. 149 (2007) 742–746.

[28] L. Ma, D. He, Top. Catal. 52 (2009) 834–844.
[29] Z. Wu, R. Jin, Y. Liu, H. Wang, Catal. Commun. 9 (2008) 2217–2220.
[30] S.J. Zhao, Y.P. Ma, Z. Qu, N.Q. Yan, Z. Li, J.K. Xie, W.M. Chen, Catal. Sci. Technol. 4 (2014) 4036–4044.
[31] H. Wang, W.F. Schneider, D. Schmidt, J. Phys. Chem. C 113 (2009) 15266–15273.
[32] B.M. Reddy, N. Durgasri, T.V. Kumar, S.K. Bhargava, Catal. Rev.–Sci. Eng. 54 (2012) 344–398.
[33] B.M. Reddy, B. Chowdhury, P.G. Smirniotis, Appl. Catal. A Gen. 211 (2001) 19–30.
[34] L. Chen, J. Li, M. Ge, J. Phys. Chem. C 113 (2009) 21177–21184.